BIOLOGY OF REPRODUCTION **82,** 1008–1017 (2010)
Published online before print 14 January 2010.
DOI 10.1095/biolreprod.109.082057

# P-Body Loss Is Concomitant with Formation of a Messenger RNA Storage Domain in Mouse Oocytes[1]

**Matyas Flemr,[4] Jun Ma,[5] Richard M. Schultz,[3,5] and Petr Svoboda[2,4]**

*Institute of Molecular Genetics,[4] Academy of Sciences of the Czech Republic, Prague, Czech Republic*
*Department of Biology,[5] University of Pennsylvania, Philadelphia, Pennsylvania*

## ABSTRACT

**In mammalian somatic cells, several pathways that converge on deadenylation, decapping, and 5′-3′ degradation are found in cytoplasmic foci known as P-bodies. Because controlled mRNA stability is essential for oocyte-to-zygote transition, we examined the dynamics of P-body components in mouse oocytes. We report that oocyte growth is accompanied by loss of P-bodies and a subcortical accumulation of several RNA-binding proteins, including DDX6, CPEB, YBX2 (MSY2), and the exon junction complex. These proteins form transient RNA-containing aggregates in fully grown oocytes with a surrounded nucleolus chromatin configuration. These aggregates disperse during oocyte maturation, consistent with recruitment of maternal mRNAs that occurs during this time. In contrast, levels of DCP1A are low during oocyte growth, and DCP1A does not colocalize with DDX6 in the subcortical aggregates. The amount of DCP1A markedly increases during meiosis, which correlates with the first wave of destabilization of maternal mRNAs. We propose that the cortex of growing oocytes serves as an mRNA storage compartment, which contains a novel type of RNA granule related to P-bodies.**

*DDX6, gene regulation, maternal mRNA, miRNA, oocyte, oocyte development, P-body, RNA granule, YBX2*

## INTRODUCTION

Transformation of a differentiated mouse oocyte into pluripotent blastomeres of the two-cell embryo (oocyte-to-embryo transition) is largely controlled by maternal mRNAs. In addition to translated mRNAs, which are very stable in the growing oocyte [1], the maternal transcriptome contains stable untranslated transcripts—dormant maternal mRNAs—that are recruited during meiotic maturation or early embryogenesis. A common mechanism regulating recruitment and stability of dormant maternal mRNAs is reversible polyadenylation that is controlled by cytoplasmic polyadenylation elements (CPEs) (reviewed in [2]). CPEs are specific sequences in 3′-untranslated regions (3′UTRs) of dormant maternal mRNAs that serve as the binding platform for the CPE-binding protein (CPEB), which controls polyadenylation-induced translation.

Cytoplasmic control of mRNA metabolism occurs within ribonucleoprotein particles (RNPs) that frequently form focal points visible by light microscopy where different pathways involved in mRNA translation control and decay are assembled. There are several classes of cytoplasmic RNA granules, such as processing bodies (P-bodies), stress granules, or germ cell granules (reviewed in [3–5]). P-bodies are cytoplasmic granules associated with repression of translation and mRNA decay. Stress granules are dense aggregates that appear in cells exposed to environmental stress and regulate translational repression and mRNA recruitment to preserve cell integrity. Germ cell granules (GCGs) are RNPs that regulate maternal mRNAs required for germ cell specification. Notably, the composition of all three types of granules overlaps to some extent. For example, the RNA helicase DDX6 (RCK/p54) and translation factor EIF4E are found in all three, whereas the decapping complex DCP1/2 is found in P-bodies and germ cell granules but not in stress granules [3, 4].

P-bodies are the most common type of RNA granules in mammalian cells. They were originally discovered as cytoplasmic foci containing 5′-3′ RNA degradation pathway protein XRN1 and the decapping complex [6–8]. Other P-body components, TNRC6 (GW182), LSM14A (RAP55), and EDC4 (also known as Ge-1 and HEDLS), were discovered in parallel when analyzing human autoimmune sera, which stained discrete cytoplasmic foci [9–11]. Subsequently, P-bodies were connected to several pathways, including nonsense-mediated mRNA decay (NMRD) and microRNA (miRNA) pathway/translational repression; P-body components represent an ever-growing list of proteins involved in RNA metabolism, including CPEB, CCR4-NOT deadenylase complex, translational repressor DDX6, translation initiation factors EIF4E and EIF4ET, and Argonaute proteins (reviewed in detail in [4, 5]).

From a structural point of view, several P-body components, such as TNRC6, EDC4, LSM14A, and DDX6 are essential for the integrity of P-bodies, and depletion of any of these proteins results in loss of P-bodies (reviewed in [4]). It has been also shown that an intact miRNA pathway is required for the formation of P-bodies [12], whereas P-bodies are not required for mRNA decay in NMRD [13]. The observation that inhibiting the miRNA pathway at any step prevents P-body formation has led to a proposal that, even though P-body components play crucial roles in mRNA silencing and decay, aggregation of the protein constituents to P-bodies is not required for miRNA function and mRNA degradation but rather is a consequence of miRNA activity [12].

RNA granules in oocytes of *Xenopus*, *Drosophila*, and *Caenorhabditis* are well characterized [14–18]. In contrast, little is known about the dynamics of RNA granules during mammalian oocyte growth and maturation. Early postnatal mouse oocytes contain granulofibrillar material reminiscent of

[1]Supported by the EMBO SDIG program, ME09039 grant, and the Purkynje Fellowship to P.S. and the NIH grant HD22681 to R.M.S.
[2]Correspondence: Petr Svoboda, Institute of Molecular Genetics, Academy of Sciences of the Czech Republic, Videnska 1083, 142 20 Prague 4, Czech Republic. FAX: 420 224310955;
e-mail: svobodap@img.cas.cz
[3]Correspondence: FAX: 215 898 8780; e-mail: rschultz@sas.upenn.edu

Received: 20 October 2009.
First decision: 9 November 2009.
Accepted: 23 December 2009.

eISSN: 1529-7268 http://www.biolreprod.org
ISSN: 0006-3363

GCGs in association with transiently appearing Balbiani bodies [19]; but the oocytes lack detectable GCGs [20]. When compared to somatic cells, mouse germinal vesicle (GV) oocytes contain markedly increased transcript levels of many components of RNA granules [21], probably a consequence of an increased demand for posttranscriptional control during the oocyte-to-embryo transition. How these factors contribute to the control of translational repression and mRNA degradation is unknown.

Here, we report an unexpected behavior of P-body proteins during mouse oocyte growth where P-bodies, present in small, meiotically incompetent oocytes, disappear and their components adopt spatially and temporarily separated functions. Moreover, the amount of DCP1A, a component of the decapping complex and a P-body-associated protein, is low during oocyte growth but displays a massive increase during meiotic maturation. In contrast, several RNA-binding proteins, including DDX6, YBX2 (MSY2), and CPEB, localize to the cortex, where they form transient RNP aggregates containing maternal mRNAs. Consistent with their function as a storage compartment, the aggregates detach from the cortex upon resumption of meiosis, relocate toward the center of the oocyte, and disperse. We propose that mouse oocytes store maternal mRNAs in a novel type of RNA granule that shares components with P-bodies.

## MATERIALS AND METHODS

### Oocyte and Embryo Collection and Culture

Oocytes and embryos were obtained from C57BL/6 mice. Meiotically incompetent oocytes were isolated from ovaries of 2- or 12-day-old mice by incubation in PBS with 1 mg/ml collagenase (Sigma) at 37°C and collected in CZB medium (Chemicon). Fully grown GV oocytes were liberated from ovaries of 6- to 14-wk-old mice by puncturing the antral follicles with syringe needles and collecting in M2 medium (Sigma) containing 0.2 mM isobutylmethylxanthine (IBMX; Sigma) to prevent resumption of meiosis. To study the role of microfilaments and microtubules, oocytes were incubated in 10 μM cytochalasin D (Sigma) in M2 with IBMX at 37°C, 5% $CO_2$ for 4 h to disrupt actin microfilaments or in 67 μM nocodazole. To obtain MII (oocyte in metaphase II) eggs and embryos, 6- to 14-wk-old mice were superovulated with 5 units of equine chorionic gonadotropin (eCG) followed by stimulation with 5 units of human chorionic gonadotropin (hCG) 48 h post-eCG; for embryo collection, the mice were mated with 8- to 20-wk-old males immediately after hCG injection. MII eggs were isolated from mice 12 h post-hCG injection by tearing the oviduct ampulla in M2 medium containing 3 mg/ml hyaluronidase (Sigma) and collected in M2 medium. Blastocysts were isolated by flushing oviducts or uteri of mice 96 h post-hCG injection. All animal experiments were approved by the Institutional Animal Use and Care Committees and were consistent with Czech laws and NIH guidelines.

### Immunofluorescent Staining

Oocytes collected in culture medium were washed briefly in PBS and fixed in 3.7% paraformaldehyde (PFA) in PBS for 1 h at room temperature (RT). Oocytes were permeabilized for 15 min in 0.1% Triton X-100 in PBS, washed extensively in blocking solution (0.01% Tween-20 and 0.1% bovine serum albumin in PBS), and incubated with the primary antibody diluted in blocking solution for 1 h. Oocyte transfer during fixation and permeabilization of oocytes was performed with a glass pipette whose inner diameter was ~250 μm.

Mouse anti-AGO2 antibody (Abnova) was used at 1:100, rabbit anti-DDX6 (Bethyl Laboratories) at 1:500, rabbit anti-DCP1A (a kind gift from Jens Lykke-Andersen) at 1:200, rabbit anti-MSY2 (YBX2) at 1:500 [22], rabbit anti-CPEB (Santa Cruz Biotechnology) at 1:100, rabbit anti-α-tubulin (Santa Cruz Biotechnology) at 1:200, human index serum 18033 (a kind gift from Marvin J. Fritzler) at 1:500, rabbit anti-eIF4a3 (a kind gift from Nahum Sonenberg) at 1:100, and rabbit anti-MATER (NLRP5, a kind gift from Jurrien Dean) at 1:1000 dilution. For AGO2 detection, the zona pellucida was removed before staining by brief incubation in acidic Tyrode solution (Chemicon) because the secondary antibody cross-reacted with the zona.

After four washes in blocking solution (10 min each), oocytes were incubated for 1 h with Alexa488- or Alexa594-conjugated secondary antibody (Invitrogen) diluted 1:500 in blocking solution. For poly(A) mRNA colocalization with proteins, 1 μM tetramethylrhodamine-oligo$(dT)_{18}$ probe (TAMRA-oligo$(dT)_{18}$; Sigma) was included in the secondary antibody mixture. Following another 4 × 10 min wash, oocytes were mounted in Vectashield with 4′, 6-diamidino-2-phenylindole (DAPI; Vector Laboratories).

### Confocal Microscopy

Fluorescent images were acquired using a Leica TCS SP5 inverted confocal laser scanning microscope equipped with HCX PL APO 40x/1.25 oil immersion objective. Sequential scanning of DAPI, fluorescein isothiocyanate (FITC) and Alexa488, and TAMRA and Alexa594 were performed by excitation using a 405-nm blue diode laser, a 488-nm argon laser, and a 561-nm helium-neon laser, respectively. The emitted light was collected in a bandwidth of 415–495 nm for DAPI, 498–578 nm for FITC and Alexa488, and 594–692 nm for TAMRA and Alexa 594. The photomultiplier tube (PMT) gain value was set at 950 V maximum, and the excitation laser intensity was adjusted to obtain a few saturated pixels in areas of the strongest signal, while keeping the signal in the control samples below detection limit. The offset was applied to cut the background signal in the space surrounding the oocytes. All the images were collected and merged using Leica LAS AF software. When better reproduction of the data in printed materials were needed, the contrast and brightness of related images were identically linearly enhanced. The original Leica acquisition files are available upon request.

### In Situ Hybridization

A modified version of Robert Singer's laboratory protocol [23] was used. Oligonucleotide probes (50-nucleotides long) were designed using Vector NTI software (Invitrogen), and the probe specificity was verified with Ensembl BlastView tool. The probe for *Mos*, that is, [Flc]AAAAGAGTAGA[FlcdT]GTCAGCTTTGGGCG[FlcdT]GGCAATCTCTCC[FlcdT]TTCAGGATCT[Flc], and the control probe targeting the EGFP-coding region, that is, [Flc]TCGATGTTG[FlcdT]GGCGGATCTTGAAGT[FlcdT]CACCTTGATGCCG[FlcdT]TCTTCTGCTT[Flc], contained 5-fluorescein (Flc) tags at the indicated positions and were obtained from Sigma. For the in situ procedure, oocytes were fixed for 1 h in 3.7% PFA in PBS at RT, washed in PBT (0.1% Tween-20 in PBS), and stored in 70% ethanol at 4°C overnight. After rehydration in PBT, oocytes were treated for 3 min with 1 μg/ml proteinase K in PBT, washed in 2 mg/ml glycine in PBT, and postfixed for 20 min in 3.7% PFA in PBT. Oocytes were initially incubated for 1 h in hybridization mix (HM; 50% formamide, 5× saline-sodium citrate [SCC] 1× Denhardt solution, 200 μg/ml yeast tRNA, 500 μg/ml salmon sperm DNA, and 2% blocking reagent [Roche]) at 37°C and then hybridized 2 h or overnight in HM with 40 nM probe at 37°C. Posthybridization washes consisted of 3 × 15 min in 30% formamide/2x SSC at 50°C, 1 × 15 min in 2x SSC at RT, and 1 × 15 min in 0.2x SSC at RT. After a wash in PBT, oocytes were either mounted in Vectashield with DAPI or incubated for 1 h in blocking solution followed by immunostaining as described in the text.

## RESULTS

### Loss of P-Bodies Early in Oocyte Growth

Because transcripts of many P-body components are overrepresented in fully grown GV mouse oocytes relative to somatic cells [21], we examined by confocal microscopy the structure of P-bodies in oocytes using antibodies against AGO2, DCP1A, and DDX6, and the human antiserum 18033 that recognizes P-body components GW182 (TNRC6 paralogs) and EDC4 [24]. *Edc4* mRNA is apparently several times more abundant than that of *Tnrc6* [21], and therefore a larger fraction of the 18033 signal may come from EDC4. Because there are no specific antibodies that distinguish the contribution of TNRC6 to the 18033 fluorescent signal, we refer to corresponding stainings as ''18033.''

Oocytes and embryos at the following developmental stages were analyzed: meiotically incompetent oocytes from 2- and 12-day-old females, fully grown GV oocytes with non-surrounded nucleolus (NSN) and surrounded nucleolus (SN) chromatin, MII eggs, and blastocysts. The SN chromatin configuration appears in the final stages of GV oocyte development and correlates with higher developmental com-

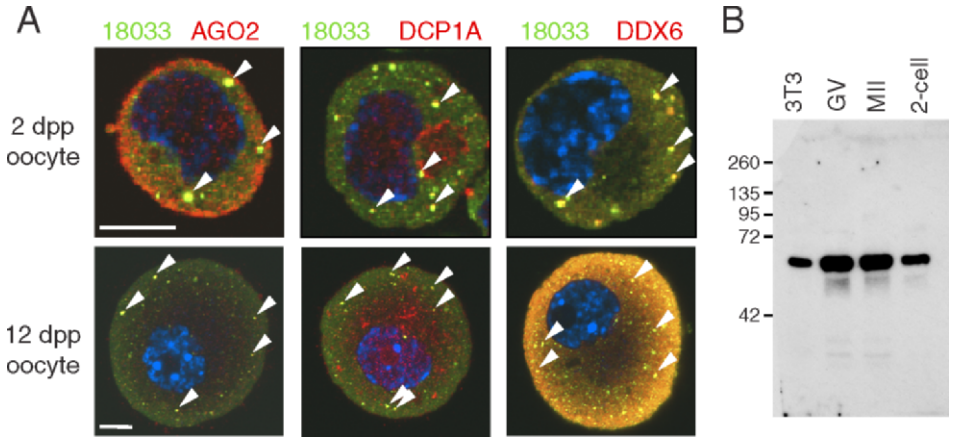


FIG. 1. P-bodies are present in small incompetent oocytes. **A**) Confocal images of mouse meiotically incompetent oocytes from 2 dpp and 12 dpp females after staining with 18033, AGO2, DCP1A, and DDX6 antibodies. Staining with 18033 is green colored, other proteins are shown in red, and DNA staining (DAPI) is shown in blue. Colocalization yields yellow color. The arrowheads depict P-bodies. For each sample, at least 10 oocytes were examined, and representative images are shown. Bar = 10 μm. **B**) DDX6 antibody specificity analyzed by Western blot analysis. DDX6 antibody used in this work detects a single band corresponding to the size of DDX6 (RCK/p54).

petence than that of oocytes with NSN chromatin, which is found during oocyte growth [25, 26]; fully grown GV oocytes with a NSN chromatin configuration complete meiosis at reduced incidence. Developmental competence is also associated with cytoplasmic factors because only 4% of SN nuclei transferred to enucleated NSN oocytes support development to the blastocyst stage [25]. Importantly, SN and NSN oocytes are isolated as a mixed population, and the NSN/SN phenotype is recognized only following staining of the DNA.

Immunostaining with antibodies recognizing AGO2, DCP1A, DDX6, and 18033 yielded bright spots of colocalizing signal in meiotically incompetent oocytes from 2 dpp (days postpartum) and 12 dpp animals (Fig. 1A). Specificity of the staining is supported by the fact that the DDX6 antibody detected only a single band in a Western blot from mouse oocytes (Fig. 1B). Thus, P-bodies are present in differentiated mouse oocytes before they enter the growth phase. Surprisingly, P-bodies were not present in fully grown GV oocytes (Fig. 2A). Detailed analysis of 12 dpp oocytes of different diameters revealed that oocytes with a diameter of ~50 μm or larger exhibited a loss of colocalization of 18033 and AGO2 (Fig. 2, B and C). Interestingly, P-bodies appeared larger in the smallest oocytes (35–40 μm) whereas in larger oocytes (~50 μm), their size decreased while more colocalizing spots were found in confocal sections (Fig. 2C).

To gain more insight into P-body dynamics, we performed immunostaining of fully grown GV oocytes, MII eggs, and early embryo stages. In fully grown GV oocytes and MII eggs, P-bodies were absent, and we found three distinct patterns (Fig. 3). AGO2 staining showed a low granular signal uniformly distributed throughout the cytoplasm of GV oocytes and MII eggs and did not colocalize with other P-body components (see also Fig. 2A). DCP1A staining of GV NSN and GV SN oocytes revealed a low uniform signal throughout the cytoplasm, which strongly increased in MII eggs, suggesting that *Dcp1a* mRNA is recruited following resumption of meiosis. DDX6 and 18033 antibodies yielded enhanced subcortical staining, which contained distinct subcortical aggregates (SCAs) in fully grown GV SN oocytes. SCAs emerged during formation of SN chromatin and disappeared during meiotic maturation, resulting in homogenous subcortical staining in MII eggs (Fig. 3). SCAs appear as domains of irregular shapes up to several micrometers in diameter and are reminiscent of stress granules. However, a component of stress granules, HuR [3], is not found in SCAs (data not shown).

It is unlikely that the staining patterns were an artifact because the same antibodies visualized P-bodies in other cell types, such as fibroblasts or cumulus cells (Fig. 3). In addition, SN oocytes and NSN oocytes were fixed and stained together, and the same patterns were reproduced in both collaborating laboratories and were observed under different fixation conditions (data not shown). Thus, our data suggest that components of dispersed P-bodies are differently regulated in growing and maturing oocytes, at least for the decapping complex (DCP1A), miRNA-mediated repression (AGO2), and translational repression (DDX6 and 18033). Notably, DDX6 and 18033 signal remained colocalized in the cortex suggesting some P-body proteins still remain functionally linked.

Finally, we analyzed early embryo stages because we hypothesized that P-bodies may assemble following zygotic genome activation when zygotic miRNAs are expressed [27]. P-bodies were found in blastocysts (Fig. 3) whereas their presence was not consistently detected in earlier embryo stages (data not shown). Taken together, our data show that P-bodies are dispersed early in oocyte growth and reappear only during later stages of preimplantation development.

### *A Novel Subcortical RNP Complex in GV Oocytes*

We next focused on the subcortical region where DDX6 and 18033 formed subcortical aggregates in GV SN oocytes (Fig. 3). A subcortical staining pattern is observed for a number of proteins, including the subcortical maternal complex (SCMC) [28] and RNA binding protein YBX2 [29].

YBX2 is a highly abundant mRNA-binding protein involved in RNA metabolism, which is essential for formation of meiotically and developmentally competent oocytes [22, 30]. Accordingly, we analyzed YBX2 colocalization with DDX6 and TNRC6/EDC4. YBX2 was detectable in P-bodies in incompetent oocytes (Fig. 4A), and we also found overlapping staining in the subcortical domain including colocalization of YBX2 and 18033 in subcortical aggregates in SN oocytes (Fig. 4B).

To test if subcortical aggregates also contain mRNA, we used the TAMRA-oligo$(dT)_{18}$ probe and found a distinct localization of the TAMRA signal in both the cytoplasm and the nucleus of NSN and SN oocytes (Fig. 4C). In NSN GV oocytes, the TAMRA signal was very high in the nucleus but lower in chromocenters. There was also a stronger perinuclear signal and an increased homogeneous subcortical staining that overlapped with YBX2 staining. In SN GV oocytes, the nuclear TAMRA signal partially overlapped with DNA staining whereas the rest of the nucleoplasm showed little or no staining. The nuclear pattern likely reflects cessation of transcription and translocation of most mRNAs to the cytoplasm during NSN and SN transition. In the cytoplasm of SN oocytes, the TAMRA signal was found in subcortical aggregates colocalizing with YBX2 (Fig. 4C).

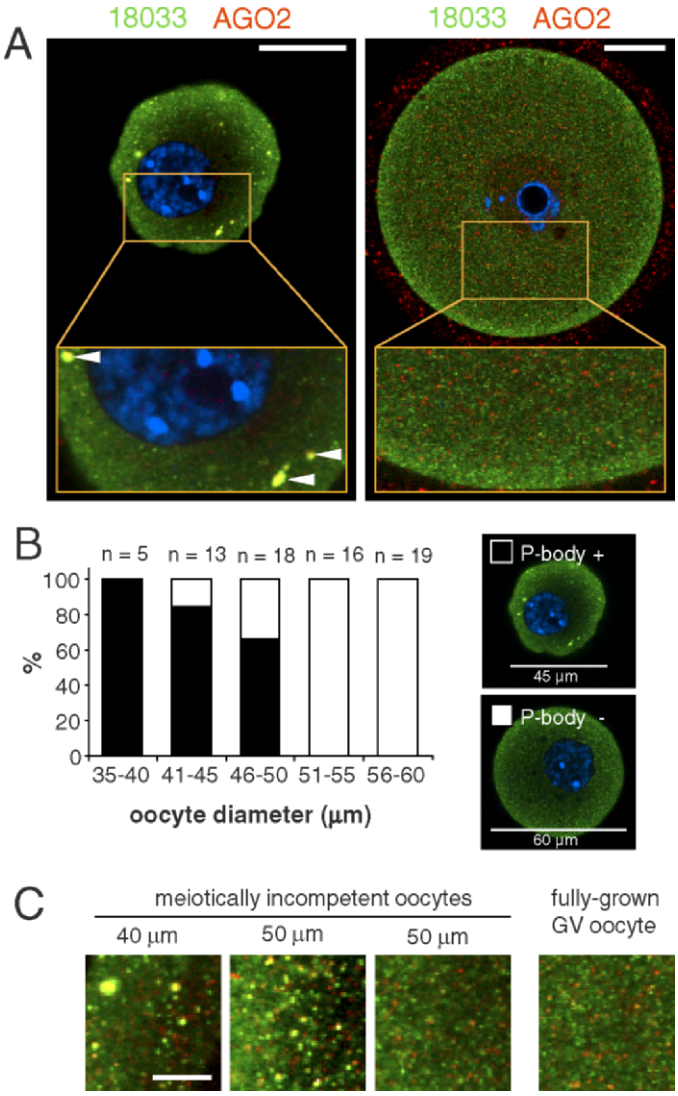


FIG. 2. P-bodies disappear as oocytes increase in size. **A**) Representative confocal images showing colocalization of 18033 and AGO2 in small, meiotically incompetent (12 dpp; left panel) and fully grown GV SN oocytes (right panel). Staining with 18033 is green colored, AGO2 is shown in red, and DNA staining (DAPI) is shown in blue. Colocalization of 18033 and AGO2 yields yellow color. Horizontal arrowheads depict P-body-like structures. AGO2 signal was enhanced in the fully grown GV oocyte to visualize the lack of AGO and 18033 colocalization. It should be noted that the observed intensity of the subcortical staining depends on setting the dynamic range of the image acquisition. Bars = 20 μm. **B**) Quantification of P-body presence/absence in incompetent oocytes (12 dpp). Oocyte diameter was estimated by image analysis of the central confocal sections. The numbers of incompetent oocytes within each group are indicated above the columns. The representative images show what was classified as a P-body-containing oocyte (shown in the solid bars in the histogram) and an oocyte not containing P-bodies (shown as the open bars in the histogram). These images were acquired in one experiment with the same confocal microscope settings. **C**) A detail of cytoplasmic staining from incompetent and fully grown oocytes showing the loss of 18033 and AGO2 colocalization in larger oocytes. Staining with 18033 is green colored, and staining with AGO2 is shown in red. Colocalization yields yellow color. Bar = 5 μm.

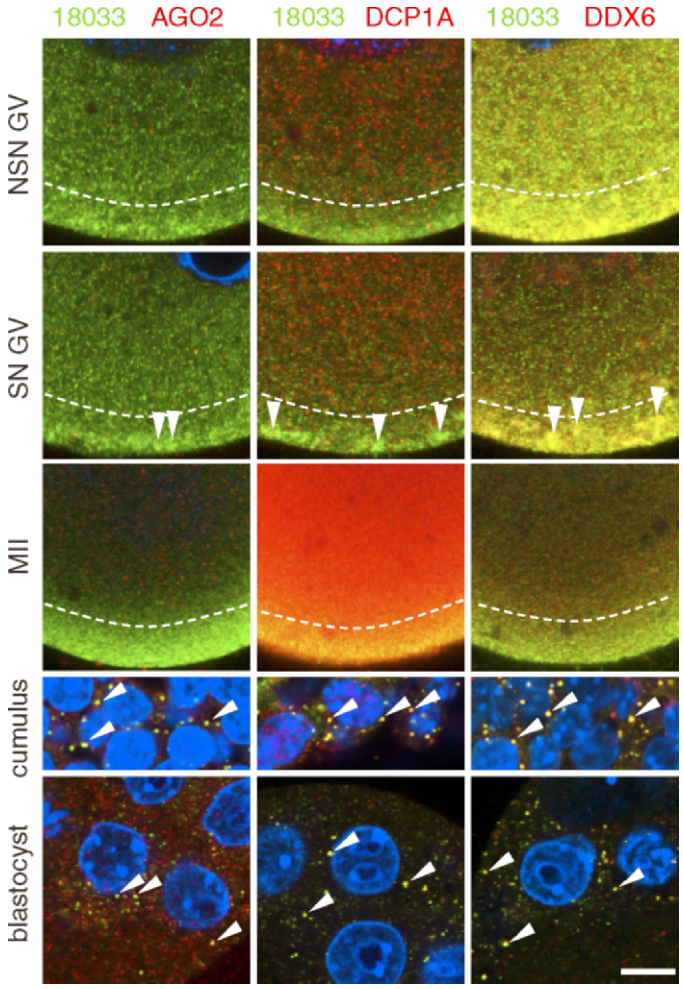


FIG. 3. Expression of P-body components during oocyte development. Confocal images of mouse GV NSN and SN oocytes, MII eggs, cumulus cells, and blastocysts after staining with 18033, AGO2, DCP1A, and DDX6 antibodies. A representative region of a whole specimen is shown. Staining with 18033 is green colored, other proteins are shown in red, and DNA staining (DAPI) is shown in blue. Colocalization yields yellow color. Diagonal arrowheads depict P-bodies in blastocysts and somatic cells. Vertical arrowheads depict subcortical aggregates found in SN GV oocytes. Dashed lines border the subcortical domain with enhanced staining of 18033 and DDX6. Note low colocalization of DDX6 and 18033 outside of the subcortical domain. Staining with the same primary antibodies were performed independently in both the United States and Czech laboratories with similar results; a representative staining is shown. GV and MII samples in each column come from the same staining experiment and were scanned with identical confocal microscope settings. SN, surrounded nucleolus; NSN, nonsurrounded nucleolus; GV, fully grown germinal-vesicle oocyte; MII, oocyte in meiosis II. Bar = 10 μm. For each sample, at least 10 oocytes, eggs, blastocysts, or cumulus cells were examined; representative images are shown.

Thus, DDX6, YBX2, 18033, and RNA define a novel compartment that we name the subcortical RNP domain (SCRD). The SCRD is apparently established in oocytes from primary follicles, and it does not mutually exclude the presence of P-bodies as evidenced by an enhanced subcortical signal of 18033 and DDX6 in populations of smaller 12 dpp oocytes (Fig. 1A). The prominent feature of the SCRD are SCAs, which appear in fully grown GV SN oocytes. The SCRD could physically interact with the SCMC complex, perhaps via OOEP (MOEP19), which is a putative RNA-binding protein [28, 31]. To test this hypothesis, we performed immunocolocalization testing of SCRD (18033) and SCMC (NLRP5) in GV SN oocytes and found little, if any, overlap of the signal in the cortex and absence of the SCMC in most of the SCAs (Fig. 5). The structural basis of SCRD is presently unclear but, like YBX2 localization [22], it does not depend on the actin or tubulin cytoskeleton (Fig. 6). Treatment of fully grown GV

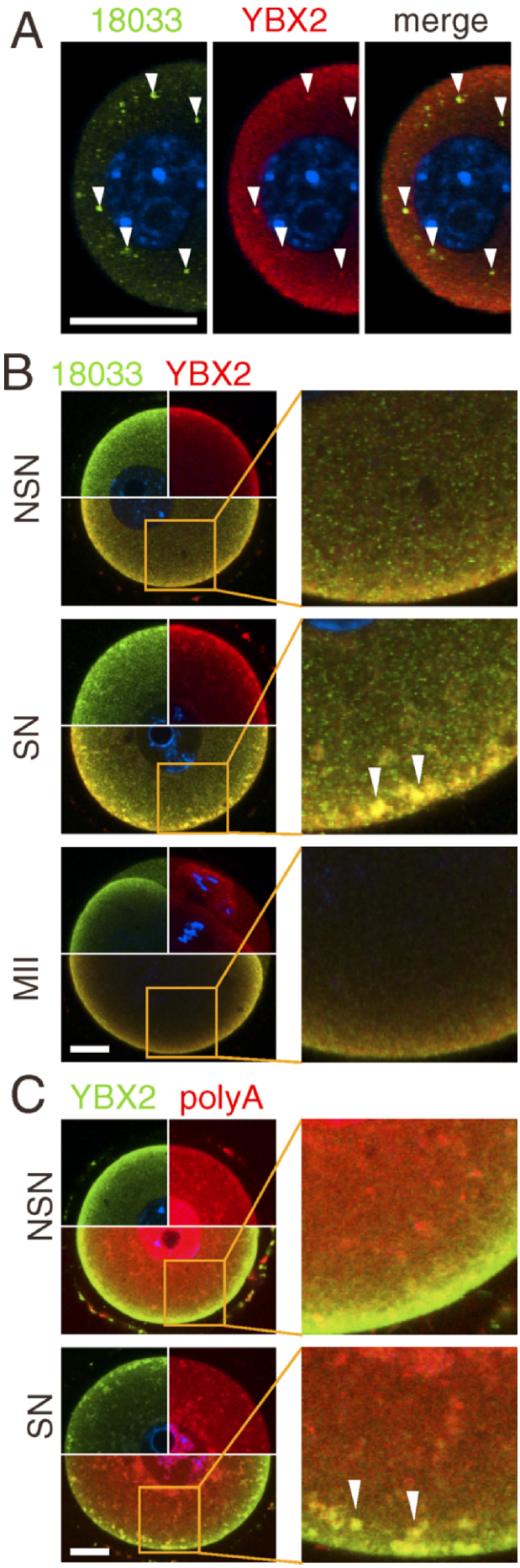


oocytes with nocodazole or cytochalasin D caused clear changes in microtubules (loss of fibrillar structures) or microfilaments (disruption of cortical actin and appearance of phalloidin-positive foci in the cytoplasm), respectively. Nevertheless, SCAs were still found intact in the cortex, and changes in DDX6 and 18033 staining patterns were not observed.

### *SCAs Store Untranslated mRNAs in the Oocyte*

One of the components of the SCRD and SCAs is the translational repressor DDX6 (Rck/p45), an ortholog of CGH-1 in *C. elegans,* Me31B in *Drosophila,* and Xp54 in *X. laevis* that is implicated in the control of maternal mRNAs in these organisms [32]. CGH-1 and its orthologs are found in a number of different RNA granules regulating mRNA stability and translation throughout the female germ cell development and in the soma [32]. We hypothesized that SCAs might also contain untranslated maternal mRNAs, such as dormant maternal mRNAs. Therefore, we performed in situ hybridization to visualize the classical dormant maternal mRNA encoding MOS kinase [33]. Indeed, *Mos* mRNA staining of SN oocytes revealed a strong subcortical staining that was concentrated into aggregates similar to SCAs (Fig. 7). We were unable to demonstrate, however, that *Mos* mRNA colocalized with SCA proteins because all attempts for in situ hybridization combined with immunofluorescent staining failed. *Mos*, like other dormant maternal mRNAs, contains a CPE, which is bound by the CPEB protein [33]. Thus, CPEB should be present in SCAs if these store untranslated maternal mRNAs. In fact, CPEB staining, which showed a slightly enhanced subcortical signal, was clearly localized to the SCAs (Fig. 7B).

Spliced mRNAs remain associated with exon junction complex (EJC) until the first round of translation. If SCAs hold translationally repressed maternal mRNAs, which were never translated, EJC components, such as EIF4A3 [34], should be also present in the SCAs. As predicted, analysis of SN oocytes identified EIF4A3 presence in SCAs (Fig. 7C), further supporting the idea of SCAs being a store of untranslated maternal mRNAs.

Finally, we addressed the behavior of SCAs upon resumption of meiosis when untranslated maternal mRNAs are recruited for translation. We found that SCAs were uncoupled from the SCRD 2 h after initiation of the germinal vesicle breakdown (GVBD) when SCAs are detached from their position close to the cytoplasmic membrane and relocated more centrally (Fig. 8). A considerable amount of 18033 and

FIG. 4. Poly(A) RNA and RNA-binding protein YBX2, but not the SCMC complex, form subcortical RNP aggregates with P-body components. **A**) YBX2 (MSY2) is also present in P-bodies. Confocal images showing colocalization of 18033 and YBX2 in small, meiotically incompetent oocytes (12 dpp). The arrowheads point to subcortical P-bodies. The blue signal is DNA staining (DAPI). **B**) Confocal images showing colocalization of 18033 and YBX2 in fully grown GV NSN and SN oocytes and MII eggs. **C**) Confocal images of colocalization of YBX2 and poly(A) RNA, visualized by TAMRA-oligo$(dT)_{18}$, in fully grown GV NSN and SN oocytes. Contrast of poly(A) samples was linearly enhanced for better presentation of colocalization in SCRD and SCAs. The identities of green and red channels are indicated above each panel, colocalization yields yellow color. The blue signal is DNA staining (DAPI). The area in the merged image outlined by solid lines is magnified in the adjacent image. The arrowheads point to subcortical RNP aggregates. For each sample, at least 10 oocytes were examined, and representative images are shown. SN, surrounded nucleolus GV oocyte; NSN, nonsurrounded nucleolus GV oocyte. Bars = 20 μm.

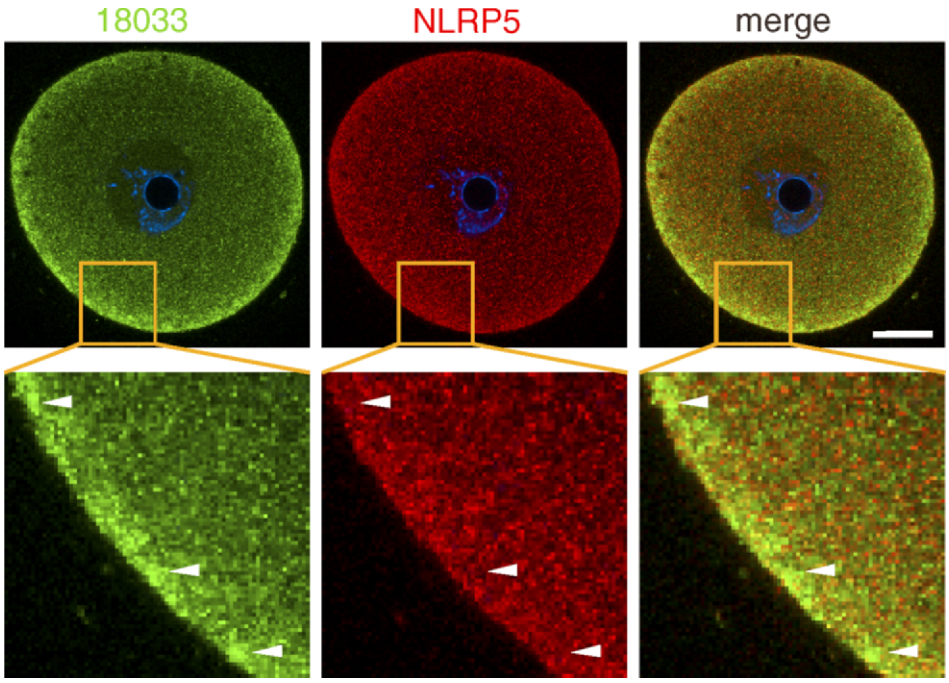


FIG. 5. Confocal images showing immunolocalization of 18033 and NLRP5 in GV SN oocytes. Identities of green and red channels are indicated above each panel, and colocalization yields yellow color. The blue signal is DNA staining (DAPI). The area in the merged image outlined by solid lines is magnified in the adjacent image. The arrowheads point to subcortical RNP aggregates. Ten oocytes were examined, and representative images are shown. SN, surrounded nucleolus GV oocyte; NSN, non-surrounded nucleolus GV oocyte. Bar = 20 μm.

DDX6 still remained in the SCRD during meiosis. SCAs assumed a more diffuse and expanded appearance during GVBD. DDX6, 18033, CPEB, EJC, and poly(A) RNA were still found in the more centrally positioned SCAs at 4 h, but not 8 h, after GVBD, while CPEB became reduced in the SCRD 4 h after GVBD (Fig. 8) and barely detectable there in MII eggs (data not shown). Thus, SCAs relocate and disintegrate in a manner consistent with release of untranslated maternal mRNAs for translation during meiosis.

## DISCUSSION

Here, we report that oocyte growth is accompanied by loss of P-bodies and subcortical accumulation of several RNA-binding proteins, including DDX6, CPEB, YBX2, and the

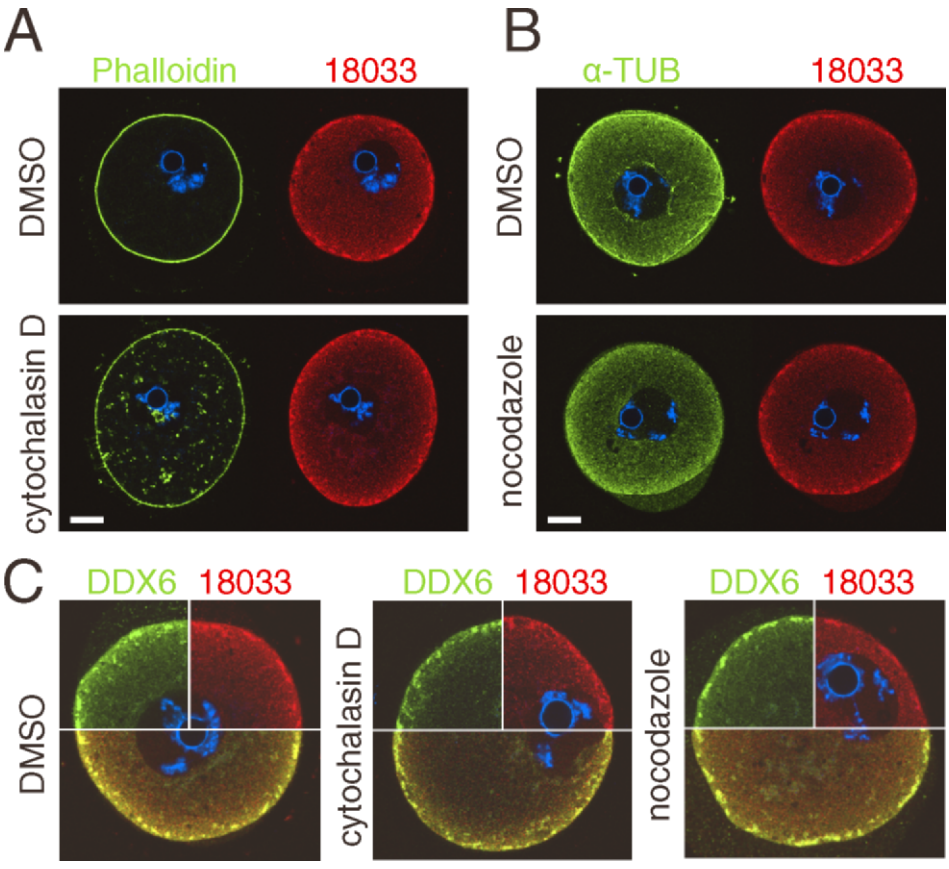


FIG. 6. SCRD and SCAs are independent on actin and tubulin cytoskeleton. **A**) Immunolocalization of 18033 and actin (Phaloidin-A488) in oocytes treated with cytochalasin D. **B**) Immunolocalization of 18033 and α-tubulin in oocytes treated with nocodazole. Staining of DNA (DAPI) is shown in blue. **C**) SCAs remain unchanged upon cytochalasin D and nocodazole treatments. Confocal images showing co-localization of 18033 and DDX6 in oocytes treated with cytochalasin D and nocodazole. Staining of DNA (DAPI) is shown in blue. Dimethyl sulfoxide (DMSO)-treated oocytes serve as a control. Bars = 20 μm.

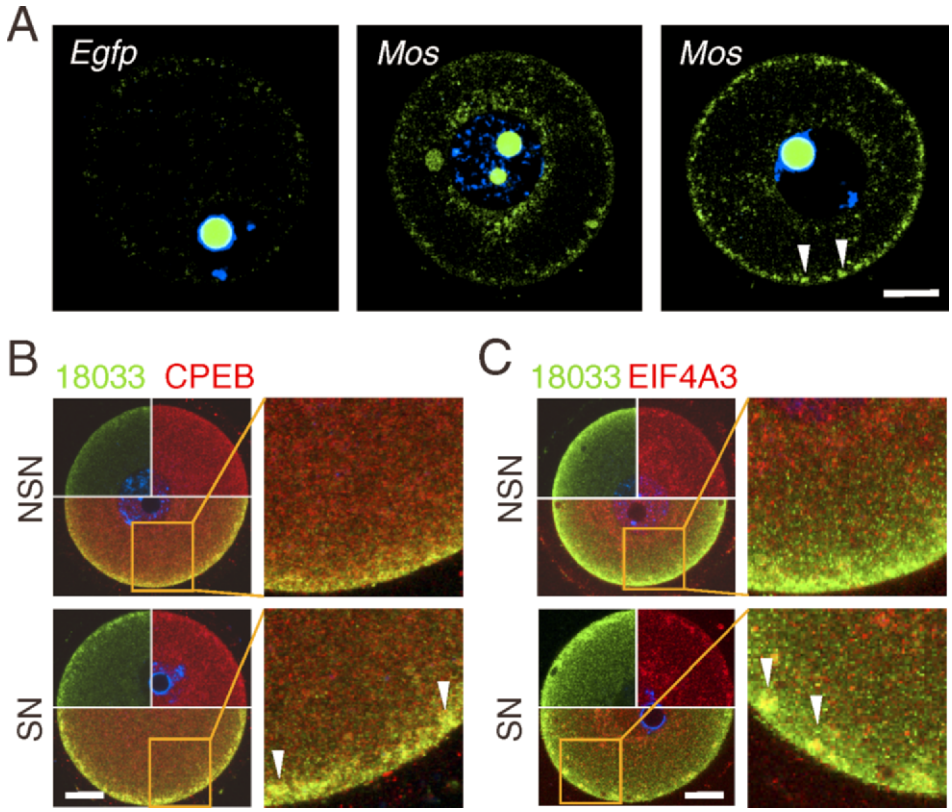


FIG. 7. Subcortical RNP domain holds dormant maternal mRNAs. **A**) In situ detection of *Mos* mRNA in the SCRD. The arrowheads depict SCA-like structures in SN oocytes, which are similar to the SCAs shown in Figures 2 and 3. Bright nucleolar signal is caused by nonspecific binding of hybridization probes. The left image shows an oocyte stained with a probe complementary to the *Egfp*-coding sequence, which served as a control for nonspecific background. For each sample, at least five oocytes were examined, and representative images are shown. **B**) Confocal images showing colocalization of 18033 and CPEB in fully grown GV SN and NSN oocytes. **C**) Confocal images showing colocalization of 18033 and EIF4A3 in fully grown GV SN and NSN oocytes. Areas in the merged images outlined by solid lines in **B** and **C** are magnified in the adjacent images. DNA staining (DAPI) is shown in blue. For each sample, at least 10 oocytes were examined, and representative images are shown. SN, surrounded nucleolus GV oocyte; NSN, nonsurrounded nucleolus GV oocyte; MII, oocyte in meiosis II. Bars = 20 μm.

exon junction complex. These proteins form transient, RNA-containing aggregates in fully grown oocytes with surrounded nucleolus chromatin configuration, which disperse during meiotic maturation. At the same time, levels of DCP1A, another P-body component, are low during oocyte growth, and DCP1A is absent in the aggregates. Abundance of DCP1A strongly increases during meiosis, which correlates with the first wave of destabilization of maternal mRNAs.

An enhanced subcortical signal has been reported for several proteins, including YBX2 [29], and DDX6 expression is detected in oocytes and early embryos [35]. The published images, however, do not have sufficient resolution to be compared with the data presented here. Interestingly, a recent report by Swetloff et al. [36] detected enhanced subcortical localization of DDX6 whereas the enhanced CPEB localization to the cortex was unclear. Our CPEB staining (Fig. 7B) shows stronger subcortical staining than the published data [36] but the overall pattern is similar; it is likely that the slightly stronger subcortical staining becomes more visible when using a wide dynamic range for image acquisition. The published DDX6 pattern [36] overlaps with the pattern for DDX6 we observe, and the slight differences may be attributed to use of a different DDX6 antibody and different dynamic range used for image acquisition.

Interestingly, Swetloff et al. [36] also reported enhanced subcortical staining for LSM14A, another P-body component [10], which is a potential additional component of the RNP complexes reported here. Because the authors focused on analysis of granules formed upon overexpression of EGFP-DCP1A, they do not comment on the subcortical localization of endogenous LSM14A and DDX6.

Our results show that P-bodies are absent from growing oocytes to early embryo stages. This result contrasts with two other studies of P-body components in oocytes and early embryos. In one study, P-body-like structures were found in two-cell embryos [37]. However, these structures were observed following overexpression of AGO2-EGFP and DCP1A-DSRED and may not reflect the normal situation.

The majority of the data reported in Swetloff et al. [36] are based on overexpressed EGFP-DCP1A in GV oocytes [36], which might result in a nonphysiological formation of P-bodies. We observed that, in contrast to the transcript level, the DCP1A protein levels are low in the oocyte and sharply rise during meiotic maturation (Fig. 3) suggesting that *Dcp1a* encodes a dormant maternal mRNA. It should be noted the DCP1A signal in MII eggs in Figure 3 is partially saturated, and when the laser power was set so that a subsaturating signal is obtained in MII eggs, the DCP1A signal becomes barely detectable in GV oocytes. Dormancy of *Dcp1a* is further supported by RNA interference (RNAi)-mediated targeting of maternal *Dcp1a* mRNA and mutation analysis of *Dcp1a* 3′UTR (Ma et al., unpublished results). In addition, YFP-tagged miRNA-targeted mRNA shows a uniform cytoplasmic distribution in fully grown GV oocytes (Ma et al., unpublished results), further suggesting that P-bodies observed upon overexpression of EGFP-DCP1A are nonphysiological. Thus, differences in behavior of endogenous and artificially expressed proteins likely account for the aforementioned inconsistencies.

The loss of P-bodies early in oocyte growth is the first case of which we are aware where P-bodies disappear from a mammalian cell under bona fide physiological conditions. Because the population of oocytes, which shows a correlation between oocyte size and the loss of P-bodies, was isolated from 12-day-old mice, the loss of P-bodies in the oocyte seems to occur during the transition between primary and secondary follicles. Although the mechanistic explanation for the loss of P-bodies is unknown, it could be related to the function of the miRNA pathway. As miRNA-mediated translational repression involves binding of TNRC6 to AGO proteins [38], the loss of

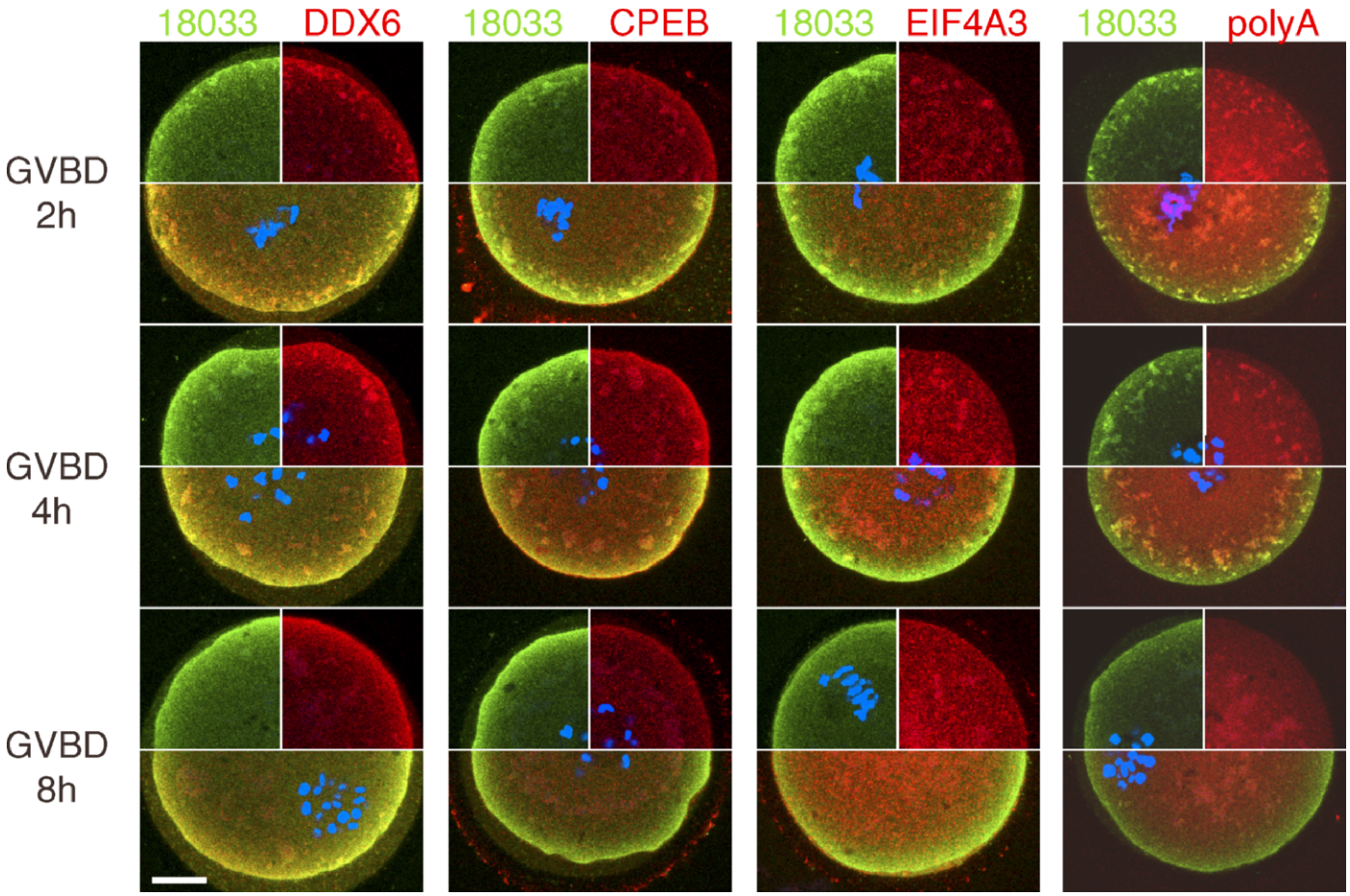


FIG. 8. Dynamics of SCRD during GVBD. Confocal images of oocytes undergoing GVBD were examined by immunofluorescent staining with 18033, DDX6, CPEB, and EIF4A3 antibodies and TAMRA-oligo(dT)$_{18}$ at 2, 4, and 8 h after release from the first meiotic block. Individual green- and red-colored stainings are shown in upper quadrants, DNA staining (DAPI) is shown in blue. The lower half of each oocyte shows a merged image where colocalization of the red and green signal yields yellow color. For each sample, at least five oocytes were examined, and representative images are shown. Bar = 20 μm.

AGO2 and 18033 colocalization at the beginning of the oocyte growth might reflect down-regulation of the miRNA pathway. In fact, results of experiments to be reported elsewhere indicate that miRNA-mediated mRNA repression is very inefficient in oocytes [39] and suggest that the meiotic failure observed in *Dicer1*$^{-/-}$ oocytes [27, 40] is due to misregulation of genes controlled by endogenous small interfering RNAs (endo-siRNAs) [41, 42] and not miRNAs [27, 43]. Moreover, maternal depletion of *Dgcr8*, which inhibits miRNA biogenesis, but not endo-siRNA biogenesis, does not result in infertility [44]. The loss of P-bodies during oocyte growth may provide the molecular underpinnings for the aforementioned results.

We show that several proteins, including P-body components DDX6, 18033, and CPEB, form a subcortical RNP domain that contains untranslated maternal mRNAs. The SCRD might represent a spatial and temporal separation of the storage function, which in P-bodies is combined with mRNA degradation [5]. The SCRD structure changes during oocyte growth, the most prominent feature being the appearance of SCAs in fully grown SN GV oocytes. The appearance of SCAs is reminiscent of stress granules, but we did not find HuR in the SCRD, thus excluding the possibility that SCAs are stress granules.

We also tested a potential link between the SCRD and the SCMC complex. The SCMC complex, which is composed of OOEP (FLOPED), NLRP5 (MATER), Filia, and TLE6 proteins, localizes to the oocyte cortex and is required during early embryo cleavage [28]. The complex has not been associated with mRNA metabolism, although OOEP is a putative RNA-binding protein [31]. Maternal loss of Filia causes defects in spindle assembly and chromosomal segregation [45]. Oocytes lacking OOEP or NLRP5 do not form the SCMC but develop normally and can be fertilized. These data indicate that the SCMC is likely not essential for maternal mRNA metabolism and is distinct from the SCRD. This notion is supported by results of our immunocytochemical experiments. Although the staining of oocytes with NLRP5 antibody is much weaker, when compared to published results, we observed increased subcortical staining, which did not co-localize well with the SCRD and, particularly, with SCAs. Furthermore, SCMC localizes to the outer cortex of preimplantation embryos where it is excluded from cell-to-cell contact regions [28], a pattern not observed for SCRD components (data not shown). Thus, similar localization of SCMC and SCRD to the cortex rather reflects a common strategy of mouse oocytes to use the cortex for deposition of mRNAs and proteins of different functions. This proposal is further supported by subcortical localization reported for DNMT1o, an oocyte-specific isoform of DNMT1, which also localizes to the cortex [46] but is functionally unrelated to maternal mRNA metabolism.

The mechanism of the SCRD and SCAs formation remains unknown. The SCRD is not lost upon disruption of actin or

tubulin cytoskeleton (Fig. 6), which also does not perturb the localization of YBX2 [22]. Unfortunately, the stability of proteins in the SCRD precluded attempts to disrupt the SCRD by RNAi. Analysis of the maternal YBX2 knockout also does not show disruption of the SCRD, suggesting that YBX2 is not an essential structural component of the SCRD (data not shown). This result is not surprising because YBX2 localization and cytoplasmic retention depends on its RNA-binding activity [22].

One of the components of the SCRD is DDX6 (Rck/p54), an ortholog of CGH-1 in *C. elegans,* Me31B in *Drosophila,* and Xp54 in *X. laevis,* that is implicated in control of maternal mRNAs in these organisms [32]. CGH-1 and its orthologs are found in a number of different RNA granules regulating mRNA stability and translation throughout the female germ cell development and in the soma [32]. The SCRD fits a model of the maternal mRNA stabilization and translational repression where CGH-1 has a conserved germline-specific role in mRNA repression and protection [17]. The subcortical localization of the SCRD perhaps denotes a suitable peripheral storage place in apparently nonpolarized mouse oocytes.

Our data offer new insights into how mRNA accumulation and assembly of mRNA decay machinery, two seemingly opposing tasks, are achieved. We propose a model in which DDX6, an unidentified 18033 antibody-interacting protein, and maternal mRNA bound by proteins such as YBX2, CPEB, and the EJC form the SCRD, a maternal mRNA storage domain, which matures into SCAs as an oocyte reaches its full developmental competence. Although growing mouse oocytes do not contain GCGs or P-bodies, the SCAs appear related to RNA storage granules observed in invertebrates [14, 15]. SCAs disperse during meiotic maturation and release maternal mRNAs, which become available for translation. While SCAs disperse, the amount of DCP1A increases and the first wave of maternal mRNA degradation begins. These data provide another example of diversity of mammalian RNA granules, which exhibit overlapping composition but different structures and functions.

## ACKNOWLEDGMENTS

We thank Jens Lykke-Andersen, Jurrien Dean, Witold Filipowicz, Marvin J. Fritzler, and Nahum Sonenberg for antibodies and Witold Filipowicz and Andrej Susor for useful discussions.

## REFERENCES

1. Brower PT, Gizang E, Boreen SM, Schultz RM. Biochemical studies of mammalian oogenesis: synthesis and stability of various classes of RNA during growth of the mouse oocyte in vitro. Dev Biol 1981; 86:373–383.
2. Richter JD. CPEB: a life in translation. Trends Biochem Sci 2007; 32: 279–285.
3. Anderson P, Kedersha N. RNA granules. J Cell Biol 2006; 172:803–808.
4. Eulalio A, Behm-Ansmant I, Izaurralde E. P bodies: at the crossroads of post-transcriptional pathways. Nat Rev Mol Cell Biol 2007; 8:9–22.
5. Parker R, Sheth U. P bodies and the control of mRNA translation and degradation. Mol Cell 2007; 25:635–646.
6. Bashkirov VI, Scherthan H, Solinger JA, Buerstedde JM, Heyer WD. A mouse cytoplasmic exoribonuclease (mXRN1p) with preference for G4 tetraplex substrates. J Cell Biol 1997; 136:761–773.
7. Ingelfinger D, Arndt-Jovin DJ, Luhrmann R, Achsel T. The human LSm1–7 proteins colocalize with the mRNA-degrading enzymes Dcp1/2 and Xrnl in distinct cytoplasmic foci. RNA 2002; 8:1489–1501.
8. van Dijk E, Cougot N, Meyer S, Babajko S, Wahle E, Seraphin B. Human Dcp2: a catalytically active mRNA decapping enzyme located in specific cytoplasmic structures. EMBO J 2002; 21:6915–6924.
9. Eystathioy T, Chan EK, Tenenbaum SA, Keene JD, Griffith K, Fritzler MJ. A phosphorylated cytoplasmic autoantigen, GW182, associates with a unique population of human mRNAs within novel cytoplasmic speckles. Mol Biol Cell 2002; 13:1338–1351.
10. Yang WH, Yu JH, Gulick T, Bloch KD, Bloch DB. RNA-associated protein 55 (RAP55) localizes to mRNA processing bodies and stress granules. RNA 2006; 12:547–554.
11. Yu JH, Yang WH, Gulick T, Bloch KD, Bloch DB. Ge-1 is a central component of the mammalian cytoplasmic mRNA processing body. RNA 2005; 11:1795–1802.
12. Eulalio A, Behm-Ansmant I, Schweizer D, Izaurralde E. P-body formation is a consequence, not the cause, of RNA-mediated gene silencing. Mol Cell Biol 2007; 27:3970–3981.
13. Stalder L, Muhlemann O. Processing bodies are not required for mammalian nonsense-mediated mRNA decay. RNA 2009; 15:1265–1273.
14. Lin MD, Jiao X, Grima D, Newbury SF, Kiledjian M, Chou TB. Drosophila processing bodies in oogenesis. Dev Biol 2008; 322:276–288.
15. Noble SL, Allen BL, Goh LK, Nordick K, Evans TC. Maternal mRNAs are regulated by diverse P body-related mRNP granules during early Caenorhabditis elegans development. J Cell Biol 2008; 182:559–572.
16. Radford HE, Meijer HA, de Moor CH. Translational control by cytoplasmic polyadenylation in Xenopus oocytes. Biochim Biophys Acta 2008; 1779:217–229.
17. Rajyaguru P, Parker R. CGH-1 and the control of maternal mRNAs. Trends Cell Biol 2009; 19:24–28.
18. Standart N, Minshall N. Translational control in early development: CPEB, P-bodies and germinal granules. Biochem Soc Trans 2008; 36: 671–676.
19. Pepling ME, Wilhelm JE, O'Hara AL, Gephardt GW, Spradling AC. Mouse oocytes within germ cell cysts and primordial follicles contain a Balbiani body. Proc Natl Acad Sci U S A 2007; 104:187–192.
20. McLaren A. Primordial germ cells in the mouse. Dev Biol 2003; 262:1–15.
21. Svoboda P. RNA silencing in mammalian oocytes and early embryos. Curr Top Microbiol Immunol 2008; 320:225–256.
22. Yu J, Hecht NB, Schultz RM. Requirement for RNA-binding activity of MSY2 for cytoplasmic localization and retention in mouse oocytes. Dev Biol 2003; 255:249–262.
23. Grunwald D, Singer RH, Czaplinski K. Cell biology of mRNA decay. Methods Enzymol 2008; 448:553–577.
24. Bloch DB, Gulick T, Bloch KD, Yang WH. Processing body autoantibodies reconsidered. RNA 2006; 12:707–709.
25. Inoue A, Nakajima R, Nagata M, Aoki F. Contribution of the oocyte nucleus and cytoplasm to the determination of meiotic and developmental competence in mice. Hum Reprod 2008; 23:1377–1384.
26. Zuccotti M, Piccinelli A, Giorgi Rossi P, Garagna S, Redi CA. Chromatin organization during mouse oocyte growth. Mol Reprod Dev 1995; 41: 479–485.
27. Tang F, Kaneda M, O'Carroll D, Hajkova P, Barton SC, Sun YA, Lee C, Tarakhovsky A, Lao K, Surani MA. Maternal microRNAs are essential for mouse zygotic development. Genes Dev 2007; 21:644–648.
28. Li L, Baibakov B, Dean J. A subcortical maternal complex essential for preimplantation mouse embryogenesis. Dev Cell 2008; 15:416–425.
29. Yu J, Hecht NB, Schultz RM. Expression of MSY2 in mouse oocytes and preimplantation embryos. Biol Reprod 2001; 65:1260–1270.
30. Yu J, Deng M, Medvedev S, Yang J, Hecht NB, Schultz RM. Transgenic RNAi-mediated reduction of MSY2 in mouse oocytes results in reduced fertility. Dev Biol 2004; 268:195–206.
31. Herr JC, Chertihin O, Digilio L, Jha KN, Vemuganti S, Flickinger CJ. Distribution of RNA binding protein MOEP19 in the oocyte cortex and early embryo indicates pre-patterning related to blastomere polarity and trophectoderm specification. Dev Biol 2008; 314:300–316.
32. Weston A, Sommerville J. Xp54 and related (DDX6-like) RNA helicases: roles in messenger RNP assembly, translation regulation and RNA degradation. Nucleic Acids Res 2006; 34:3082–3094.
33. Gebauer F, Richter JD. Mouse cytoplasmic polyadenylylation element binding protein: an evolutionarily conserved protein that interacts with the cytoplasmic polyadenylylation elements of c-mos mRNA. Proc Natl Acad Sci U S A 1996; 93:14602–14607.
34. Chan CC, Dostie J, Diem MD, Feng W, Mann M, Rappsilber J, Dreyfuss G. eIF4A3 is a novel component of the exon junction complex. RNA 2004; 10:200–209.
35. Matsumoto K, Kwon OY, Kim H, Akao Y. Expression of rck/p54, a DEAD-box RNA helicase, in gametogenesis and early embryogenesis of mice. Dev Dyn 2005; 233:1149–1156.
36. Swetloff A, Conne B, Huarte J, Pitetti JL, Nef S, Vassalli JD. Dcp1-bodies in mouse oocytes. Mol Biol Cell 2009; 20:4951–4961.
37. Lykke-Andersen K, Gilchrist MJ, Grabarek JB, Das P, Miska E, Zernicka-Goetz M. Maternal Argonaute 2 is essential for early mouse development at the maternal-zygotic transition. Mol Biol Cell 2008; 19:4383–4392.
38. Eulalio A, Huntzinger E, Izaurralde E. GW182 interaction with Argonaute

is essential for miRNA-mediated translational repression and mRNA decay. Nat Struct Mol Biol 2008; 15:346–353.
39. Ma J, Flemr M, Stein P, Berninger P, Malik R, Zavolan M, Svoboda P, Schultz RM. MicroRNA activity is suppressed in mouse oocytes. Curr Biol 2010; 20:265–270.
40. Murchison EP, Stein P, Xuan Z, Pan H, Zhang MQ, Schultz RM, Hannon GJ. Critical roles for Dicer in the female germline. Genes Dev 2007; 21: 682–693.
41. Tam OH, Aravin AA, Stein P, Girard A, Murchison EP, Cheloufi S, Hodges E, Anger M, Sachidanandam R, Schultz RM, Hannon GJ. Pseudogene-derived small interfering RNAs regulate gene expression in mouse oocytes. Nature 2008; 453:534–538.
42. Watanabe T, Totoki Y, Toyoda A, Kaneda M, Kuramochi-Miyagawa S, Obata Y, Chiba H, Kohara Y, Kono T, Nakano T, Surani MA, Sakaki Y, Sasaki H. Endogenous siRNAs from naturally formed dsRNAs regulate transcripts in mouse oocytes. Nature 2008; 453:539–543.
43. Kaneda M, Tang F, O'Carroll D, Lao K, Surani MA. Essential role for Argonaute2 protein in mouse oogenesis. Epigenetics Chromatin 2009; 2:9.
44. Suh N, Baehner L, Moltzahn F, Melton C, Shenoy A, Chen J, Blelloch R. MicroRNA function is globally suppressed in mouse oocytes and early embryos. Curr Biol 2010; 20:271–277.
45. Zheng P, Dean J. Role of Filia, a maternal effect gene, in maintaining euploidy during cleavage-stage mouse embryogenesis. Proc Natl Acad Sci U S A 2009; 106:7473–7478.
46. Doherty AS, Bartolomei MS, Schultz RM. Regulation of stage-specific nuclear translocation of Dnmt1o during preimplantation mouse development. Dev Biol 2002; 242:255–266.